This report is composed of two manuscripts: "TaC as a Diffusion Barrier Between Si and Cu" (submitted to Journal of Applied Physics) and "Amorphous Layer Formation at the TaC/Cu Interface in the Si/TaC/Cu Metallization System" (submitted to Applied Physics Letters).
Copyright 2001, authors and American Institute of Physics.

Stability of TaC Diffusion Barrier Between Si and Cu

Tomi Laurila, Kejun Zeng, and Jorma K. Kivilahti

Laboratory of Electronics Production Technology, Helsinki University of Technology, P.O. Box 3000, FIN-02015 HUT, Finland

Jyrki Molarius and Ilkka Suni

VTT Microelectronics, FIN-02044 VTT, Finland

ABSTRACT

The reaction mechanisms and related microstructures in the Si/TaC/Cu metallization system have been studied experimentally and theoretically by utilizing ternary Si-Ta-C, Ta-C-Cu and Ta-C-O phase diagrams as well as calculated activity diagrams. With the help of sheet resistance measurements, Rutherford backscattering spectrometry, x-ray diffraction, scanning electron microscopy, and transmission electron microscopy, the metallization structure with the 70 nm thick TaC barrier layer was observed to fail completely at temperatures above 725 °C because of the formation of large Cu_3Si protrusions. However, the formation of amorphous Ta layer containing significant amounts of carbon and oxygen was already observed at the TaC/Cu interface at 600 °C. This layer also constituted an additional barrier layer for Cu diffusion, which occurred only after the crystallization of the amorphous layer. The formation of Ta_2O_5 was observed at 725 °C with x-ray diffraction, indicating that the oxygen rich amorphous layer had started to crystallize. The formation of SiC and $TaSi_2$ occurred almost simultaneously at 800 °C. The observed reaction structure was consistent with the thermodynamics of the ternary systems. The metallization structures with 7 nm and 35 nm TaC barrier layers failed above 550 °C and 650 °C, respectively, similarly because of the formation of Cu_3Si. The high formation temperature of $TaSi_2$ and SiC implies high stability of Si/TaC interface, thus making TaC layer a potential candidate to be used as a diffusion barrier for Cu metallization.

I. INTRODUCTION

As dimensions of solid state devices are scaled down, the continuing demand for improvement in the performance of interconnects has led to the need to replace currently used aluminum based conductors with materials that have better electrical properties. Moreover, the reliability of aluminum based conductors is limited by the relatively poor electromigration resistance of the material. Copper has attracted increasing attention as a "state-of-the-art" metallization material because of its better electrical properties as well as better electromigration resistance in comparison to aluminium.[1,2] Unfortunately, the interaction between Si and Cu is strong and detrimental to the electrical performance of Si even at temperatures below 200 °C.[3-6] Therefore, it is necessary to implement a barrier layer between Si and Cu. Ta and Ta-based diffusion barriers have been the subject of numerous investigations.[7-17] They fulfill rather well the overall requirements for diffusion barriers as summarized by Nicolet.[18] Among the most promising candidates to be used for this purpose are the binary tantalum nitrides and carbides. Whereas Ta-nitrides have been investigated widely, only few known reports have been published about TaC- based diffusion barriers.[16,17] Hence, there is a clear need for further investigation of these diffusion barrier layers, since they seem to offer a viable solution to the barrier layer problem associated with Cu metallization.

There exist two stable carbides in the Ta-C system, Ta_2C and TaC, with melting points of 3330 °C and 3985 °C, respectively.[19] Since both carbides are interstitial compounds and thermally very stable[20], the stability of Si/TaC interface, as compared for example to Si/Ta interface, is expected to increase because of the elevated formation temperature of tantalum silicides. Further, because no stable carbides exist in the Cu-C system, the interface between TaC and Cu should be stable. Moreover, based on the evaluated Ta-C-Cu ternary phase diagram, Cu is in thermodynamic equilibrium with both carbides.[21] However, Cu is eventually expected to penetrate through the barrier layer owing to its high affinity towards Si. Thus, the failure mechanism is most likely a combination of tantalum silicide formation at Si/TaC interface and diffusion of Cu through the barrier layer with accompanied Cu_3Si formation at the same Si/TaC interface.

In the present study, the reactions in the Si/TaC/Cu metallization system are investigated experimentally and theoretically by utilizing a combined thermodynamic-kinetic approach. Although the complete thermodynamic equilibria are hardly ever encountered in thin film systems, the local equilibrium is, however, generally attained at interfaces. Therefore, the phase diagrams provide us with an efficient method for designing diffusion barrier layers between various metallizations, especially when they can be combined with kinetic information. The phase relations in the system are examined by combining the assessed binary data into ternary thermodynamic descriptions. By employing the same thermodynamic data activity diagrams will also be calculated. The information extracted from these diagrams are used together with the experimental results obtained to discover the underlying mechanism(s) for the failure. It is expected that by employing this approach better understanding of the equilibria and reactions in the system is achieved.

II. EXPERIMENT

The copper and tantalum carbide films were sputtered onto cleaned and oxide-stripped (100) n-type Si substrates in a dc/rf-magnetron sputtering system. The deposition of TaC was obtained from the TaC-target (hot-pressed, 6.2 wt-% of C, main impurity Nb ~ 0.3 wt-%) in argon atmosphere. The pressure before the deposition runs was approximately 10^{-5} Pa. The thickness of the tantalum carbide layers was 70 nm. The copper films with thickness of 400 nm were subsequently sputter-deposited without breaking the vacuum. In order to investigate the effect of the barrier thickness on the stability of the metallization structure, another set of samples with thinner tantalum carbide (7 nm and 35 nm) and copper layers (100 nm) were fabricated. The samples were annealed under the vacuum of 10^{-4} Pa at temperatures ranging from 500 °C to 800 °C for 30 minutes.

The sheet resistance measurements at room temperature by using a four-point probe were used to detect possible interfacial reactions after the each annealing step. The reaction products in the Si/TaC/Cu metallization schemes were characterized by x-ray diffraction (XRD), Rutherford backscattering spectrometry (RBS) and the transmission electron microscopy (TEM). Surfaces of the samples were also examined with an optical microscope and scanning electron microscope (SEM). XRD analyses were conducted with a Bruker axs D8 Advance diffractometer. Both fixed 1deg. incoming angle and theta-2theta

measurements were carried out with a measurement range of 20-60 ° (2θ). The RBS measurements were performed with a 2 MeV He+ ion beam normal to the surface, with a scattering angle of 170 °. The TEM investigations were conducted with JEOL 2000FX analytical TEM/STEM operated at 200 kV. A few micrographs were taken also at 400 kV acceleration voltage (JEM-4010). SEM investigations were performed with a JEOL JSM-6335F field emission scanning electron microscope operated at 15 kV. The results of the experimental investigations were compared with the assessed phase diagrams. Ternary Si-Ta-C, Ta-C-Cu and Ta-C-O phase diagrams as well as the corresponding activity diagrams were evaluated from the assessed binary thermodynamic data.

III. RESULTS

The sheet resistance of the layered metallization structure as a function of temperature is displayed in Fig. 1.

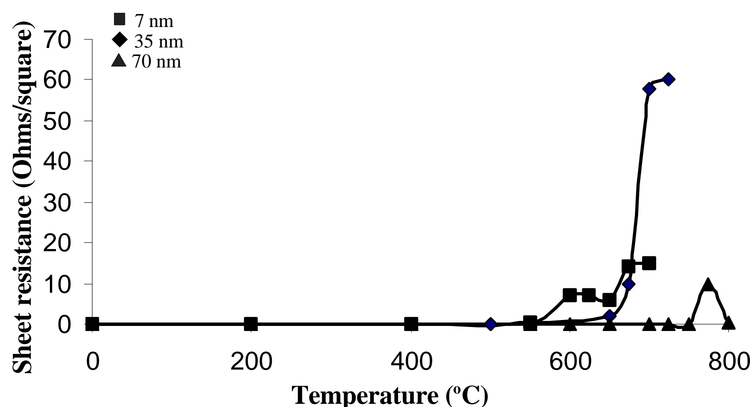

Fig. 1. Sheet resistance vs. temperature curve of the Si/TaC/Cu metallization structures with different TaC layer thickness annealed for 30 min at different temperatures.

At 775 °C there is an abrupt rise in the curve of the sample with the 70 nm thick TaC film, showing that some reaction has occurred in the metallization system. Above 775 °C, the sheet resistance starts to decrease. Thus, the structure behaves like an intrinsic semiconductor. This suggests that reaction products with high resistivity have been formed, since the underlying silicon is now carrying almost the entire probe current. The thin 7 nm

and 35 nm TaC layers are stable up to 550 °C and 650 °C, respectively, as determined by the sheet resistance measurements (Fig. 1). It must be realized, however, that the sheet resistance measurements monitor chiefly the state of the Cu overlayer, since it carries almost the entire probe current. Thus, interaction between other layers, e.g. TaC and Si, may not be immediately detected with this technique.

The surfaces of the thick (70nm) samples maintain a shiny copper-like appearance up to 750 °C and the 7 nm and 35 nm samples up to 550 °C and 650 °C, respectively. The SEM micrograph of the surface structure of the sample with 70 nm thick TaC barrier annealed at 800 °C is shown in Fig. 2. As can be seen, large "squares" (approximately 20-30 μm in diagonal) have formed on the surface. These defects seem to be composed totally out of one phase. There is also comparable phase distributed around the central "square" in Fig. 2, as pointed out by the similar contrast (represented by an arrow in Fig. 2). These "squares" are surrounded by a "flowery" patterned structure, which seems to be a two phase structure where one phase is embedded into the other. Some of this "flowery" pattern can also be seen inside the large "squares". The structures seen on the surface of the samples are similar to those observed earlier to be associated with the failure of the Ta barrier layers and the formation of Cu_3Si and $TaSi_2$.[22]

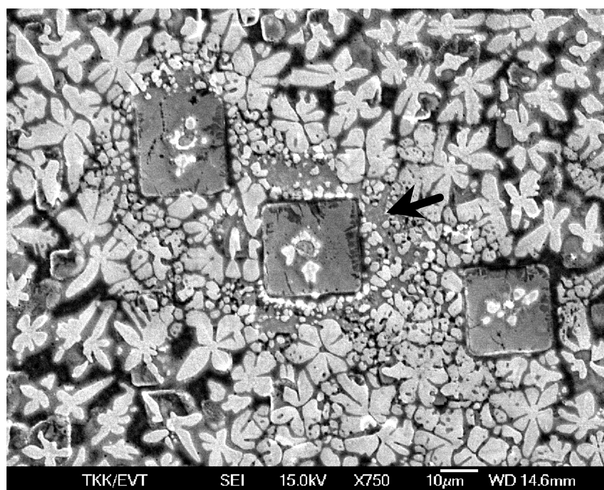

Fig. 2. SEM micrograph from the surface of the Si/TaC(70nm)/Cu(400nm) sample annealed at 800 °C for 30 min. The arrow shows the phase around the "squares" which seems to be the same as the bulk of the individual "squares".

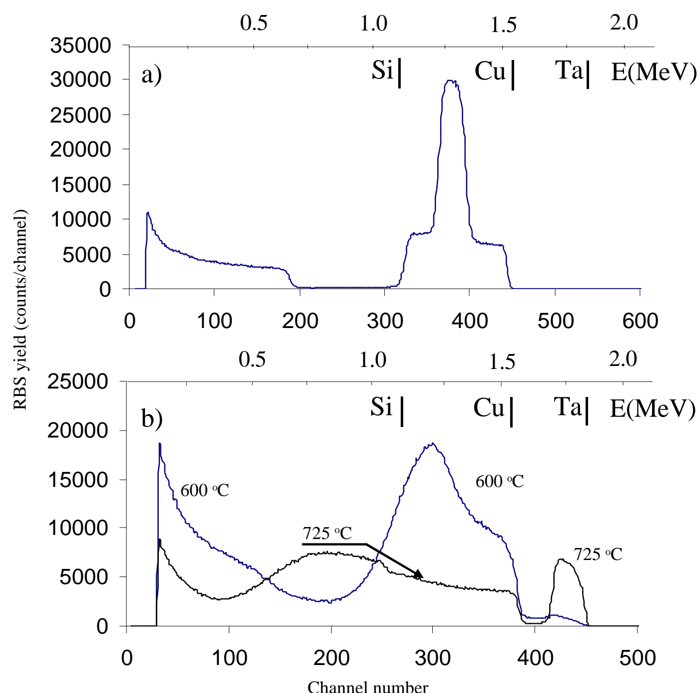

Fig. 3. RBS spectra (2.0 MeV 4 He^+, θ = 170 °) from the Si/TaC(70nm)/Cu(400nm) samples a) no annealing and b) annealed at different temperatures for 30 min. Vertical arrows represent surface scattering energies.

The RBS analyses of the as-deposited samples show sharp edges of the elements in the spectra, thus showing no intermixing between the layers before the annealings (Fig. 3 a). Fitting the measured RBS data to GISA 3.99 simulations[23,24] reveals that the TaC layer thicknesses are 7 nm, 35 nm and 70 nm for the three types of sample, respectively. The thicknesses were obtained by using the bulk atomic densities. The composition of the Ta-C layers is slightly rich with respect to carbon, $Ta_{48}C_{52}$. Even when taking into account errors in the measurements and in the simulations,[24] this deviation can not be attributed solely to experimental error. Shifts in stoichiometry in TaC have been observed to take place only towards the Ta-rich side (i.e. C defiant carbides)[20], and therefore the slight excess of carbon implies that graphite precipitation may occur during the annealings. RBS measurements of the annealed samples showed clearly discrete layers with no intermixing up to 550 °C. However, at 600 °C the RBS spectrum suggests that interdiffusion of Ta and Cu takes place (Fig. 3 (b)). As can be seen, some tantalum moves to the surface. In addition the trailing edge of the Cu and leading edge of the Si signals are smoothened, suggesting some

intermixing. The temperature where the degradation of the layers starts according to the RBS is unexpectedly low. However, if the slight excess of carbon in the TaC films results in segregation to the grain boundaries as expected, this may open short circuit diffusion paths for Cu and Si atoms via the most likely amorphous graphite media located in the grain boundaries. Similar failure mechanism in carbon rich TaC films was also suggested by Imahori *et.al.*[16] Moreover, the TaC films are expected to contain pinholes and other defects, which may enable interdiffusion locally at considerably low temperatures. Therefore, despite the overall stability of the TaC layers, it seems that the layers have weak spots where the mixing occurs already at low temperatures. From the backscattering spectra taken at higher temperatures, for example at 725 °C, it is very difficult to obtain more information about the reactions taking place, since the spectra become quite complex. Nevertheless, as can be seen from Fig. 3, more Ta moves to the surface and the Cu and Si interfaces degrade further, showing more severe intermixing.

In order to obtain more information about the phase formation during the annealings, XRD analyses were carried out. Both fixed 1 deg. incoming angle and theta-2theta configurations were used. The results shown are a combination of both types of measurements. The analyses show that up to 725 °C only TaC and Cu are present in the samples with the 70 nm TaC barrier layer (see Fig. 4). Further, no reaction products are detected at 600 °C with XRD. At 725 °C there are some diffractions from Ta_2O_5, denoting the presence of oxygen in the annealing environment and in the films themselves. At 750 °C, the formation of copper silicide, Cu_3Si, takes place according to the XRD. However, the analyses show that the structure of the Cu_3Si is not equilibrated, since the peaks are not "stable", *i.e.* they change their position slightly with changing temperature. This can be explained by the fact that Cu_3Si has at least three crystal structures stable in different temperature ranges[19,25,26], and the given phase may still be in tranformation. Moreover, it has been observed earlier that the peak positions change slightly if the samples are kept at room temperature for a prolonged time.[25] No other silicides are detected at this temperature with XRD. At 800 °C, the TaC, Cu, and Ta_2O_5 peaks disappear, and only Cu_3Si and $TaSi_2$ peaks are present. The samples with the 7 nm TaC barrier layer show only Cu peaks up to 550 °C (Fig. 5). The reason for this is most likely that the very thin (7 nm) TaC layer is in nanocrystalline (*i.e.* nearly amorphous) state.

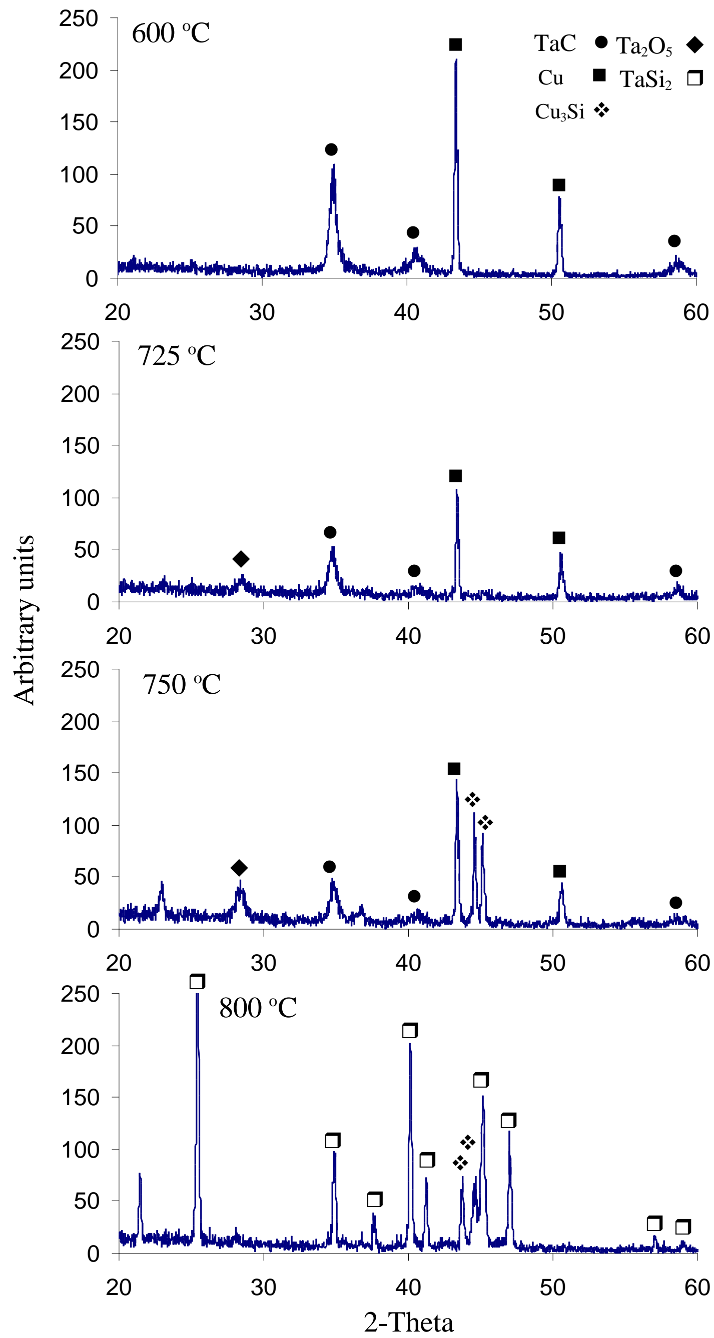

Fig.4. XRD spectra from the Si/TaC(70nm)/Cu(400nm) samples annealed for 30 min at different temperatures.

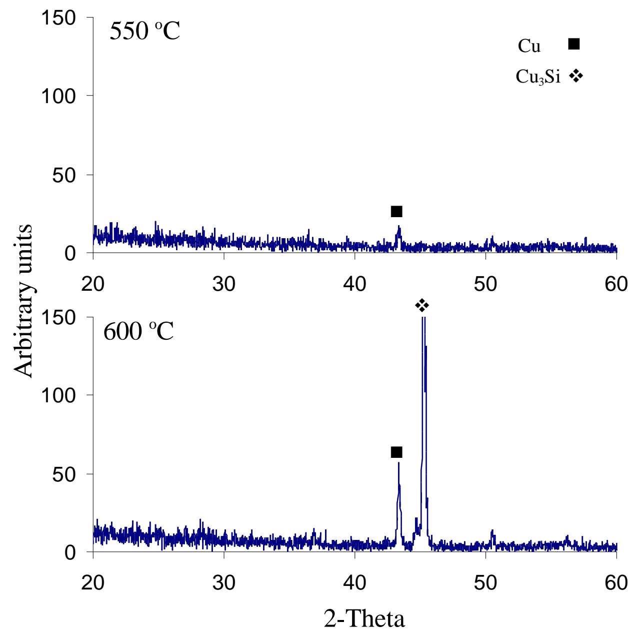

Fig.5. XRD spectra from the Si/TaC(7nm)/Cu(100nm) samples annealed for 30 min at different temperatures.

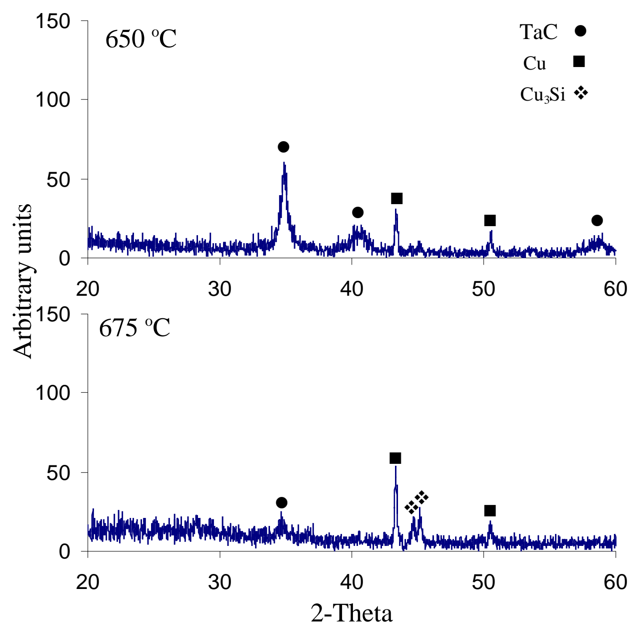

Fig.6. XRD spectra from the Si/TaC(35nm)/Cu(100nm) samples annealed for 30 min at different temperatures.

Similar results indicating the amorphous nature of sputter-deposited TaC films have similarly been reported by Tsai *et al.*[17] The formation of Cu_3Si occurs at 600 °C in these samples as displayed in Fig. 5. The samples with the 35 nm TaC barrier layer show both TaC and Cu peaks up to 650 °C (Fig. 6). The formation of Cu_3Si takes place at 675 °C. At the temperature of formation of Cu_3Si, there is still some TaC left in the 35 nm sample. No trace of $TaSi_2$ is found in the thin 7 nm and 35 nm samples annealed up to 700 °C and 725 °C, respectively. Despite the different thicknesses of the films, the failure seems to be induced by Cu penetration through the TaC layer and the formation of Cu_3Si, at least according to the XRD analyses. The Si/TaC interface is relatively stable, since no reaction is observed below 800 °C.

To clarify the puzzling RBS results from the samples annealed at 600 °C a cross-sectional TEM analysis was performed. The view from the 70 nm thick sample annealed at 600 °C for 30 minutes is presented in Fig. 7, which shows unambiguously the presence of an amorphous layer between TaC and Cu. The amorphous structure of the interlayer can be seen more clearly from the high resolution micrograph presented in Fig. 8.

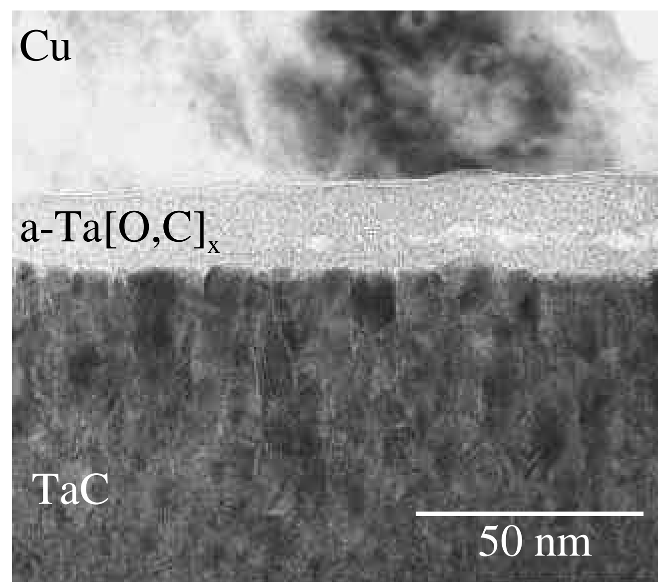

Fig.7. Bright field TEM micrograph from the Si/TaC(70nm)/Cu(400nm) sample annealed at 600 °C for 30 min.

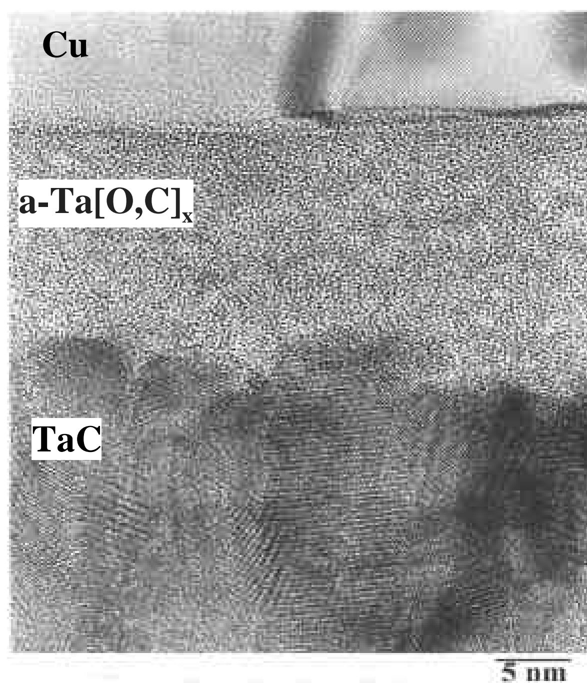

Fig.8. HREM micrograph from the amorphous $Ta[C,O]_x$ phase from the sample annealed at 600 °C for 30 min.

The amorphous nature of the layer was further confirmed with electron diffraction patterns (not shown here). The composition of the layer was analyzed from the very thin foil (tens of nanometers thick) with the energy dispersive spectroscopy (EDS) in the analytical TEM to be Ta with noticeable amounts of oxygen and carbon. As high amounts of oxygen and carbon were present only within the amorphous layer. The layer is most probably $Ta[O,C]_x$ (i.e. metastable oxide) containing some carbon released from the partly dissociated TaC layer. The amorphous layer also explains why the XRD was unable to detect reaction product formation at 600 °C and gives some indication why the RBS spectrum had already degraded at 600 °C.

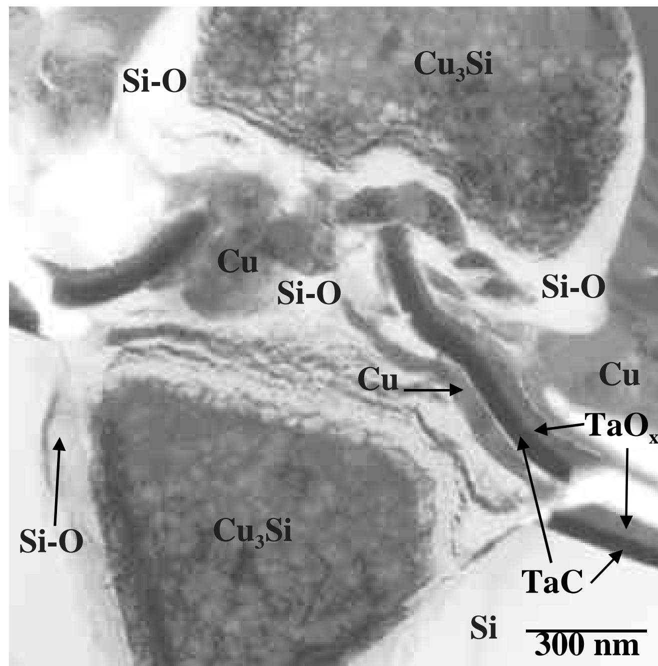

Fig.9. Bright field TEM micrograph from the Si/TaC(70nm)/Cu(400nm) sample annealed at 750 °C for 30 min.

The XTEM micrograph of the sample with a 70 nm TaC barrier layer annealed at 750 °C for 30 minutes is shown in Fig. 9. Here, one can clearly see the formation of large triangular grain, which was identified with the combination of the EDS and the electron diffraction analyses as slightly Si defiant Cu_3Si phase. The size of the protrusion is considerably smaller than observed from the sample annealed at 800 °C (see Figs. 2 and 11), indicating that the reaction continues to advance and the defect is expected to grow. It is evident from the micrograph that the phase has a cellular appearance, but the origin of this is not yet clear. The cellular structure may be a result of the fact that Cu_3Si is still under microstructural evolution, as mentioned above. The hemispherical grain above the triangular grain was identified as Si deficient Cu_3Si, again with the similar cellular appearance. These two defects will most probably "combine" at higher temperatures (~ 800 °C) by conventional Ostwald ripening to form the observed larger defects. Between these two grains, there is a region composed of Si-O, Cu-Si, and Ta-rich phases. The Ta-rich film shown in Fig. 9 is actually a 2-phase structure with TaC at the bottom of the film and crystalline TaO_x phase (expected to be Ta_2O_5 as detected also with the XRD) at the upper part of the film. There are also some remains from the Cu film between the two Cu_3Si

grains, as suggested by the XRD analysis taken at the same temperature (see Fig.4). No continuous TaC film is seen in this micrograph, which suggests that the rupture of the barrier layer has taken place. However, as can be seen from the micrograph taken at the same temperature from a different location (Fig. 10), the TaC/TaO_x bilayer is still present at other sites. The formation of the Cu_3Si protrusion seen in the micrograph occurs because of the diffusion of Cu through the barrier most probably via the grain boundaries of the TaC layer. The crystalline nature of the bilayered structure is also clearly seen in this micrograph.

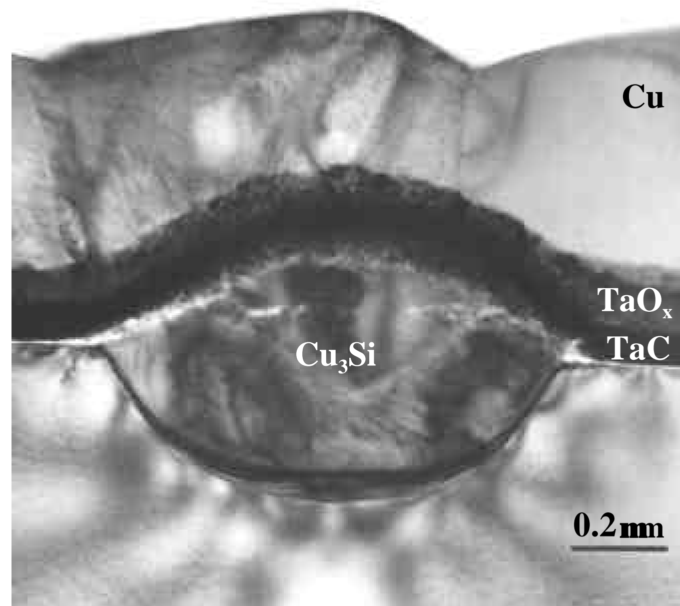

Fig.10. Bright field TEM micrograph from the Si/TaC(70nm)/Cu(400nm) sample annealed at 750 °C for 30 min.

In Fig. 11, an "overall" view of the TEM cross-section of the sample annealed at 800 °C through one of the "squares" and the "flowery" pattern (see Fig. 2) is presented. The cross-section is inverted (vertically), thus the original top surface seen in Fig. 2 is at the bottom in this micrograph.

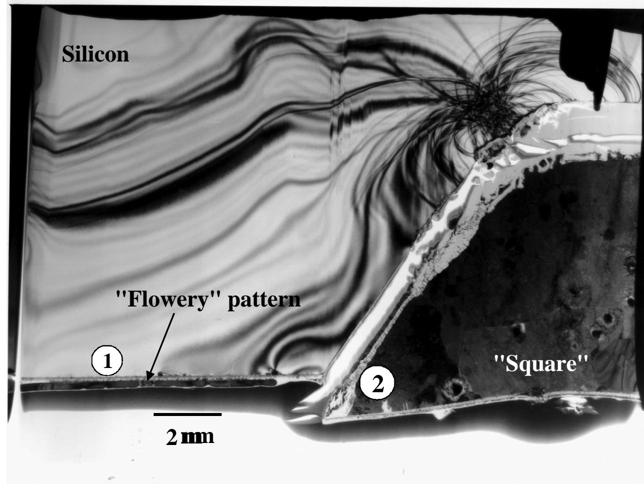

Fig. 11. Bright field TEM micrograph from the Si/TaC(70nm)/Cu(400nm) sample annealed at 800 °C for 30 min.

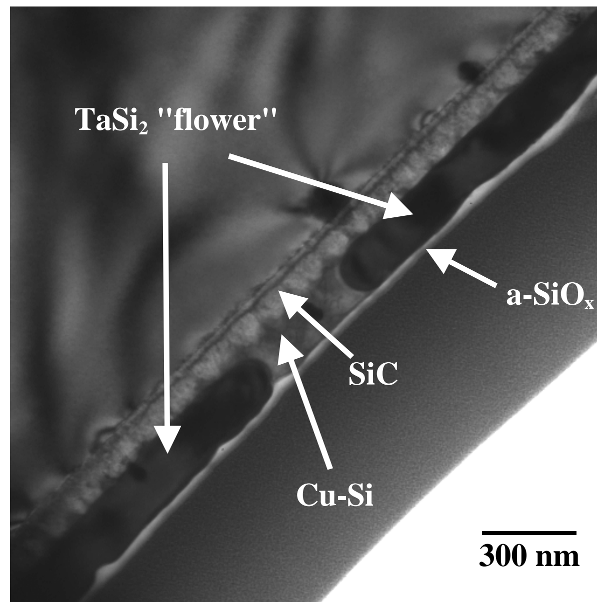

Fig.12. Bright field TEM micrograph from the Si/TaC(70nm)/Cu(400nm) sample annealed at 800 °C for 30 min corresponding to ① in Fig.11.

A more detailed, magnified view of the area marked as ① in Fig. 11 can be seen in Fig. 12. It shows that the "flowery" pattern seen from the top in Fig. 2 is in fact $TaSi_2$, as determined by a combination of elemental analyses with the EDS and diffraction pattern analysis. However, the overall structure of the reaction product layers is somewhat complex. On the

top surface, there is a very thin amorphous SiO_x layer. Below this top layer are the $TaSi_2$ grains. Between the two $TaSi_2$ grains seen in the micrograph, there is a Cu-rich region that contains some Si. This was expected to be Cu_3Si, but it was not possible to confirm it unambiguously owing to the very small amount of the phase present. This is the phase that can be seen from the top in Fig. 2 around the central "square" (the arrow in Fig. 2) and is considered to be the same phase as the "squares" themselves. Below the $TaSi_2$ grains, there is again the same Cu-rich layer that was observed between the $TaSi_2$ grains. Beneath this layer, there is another layer composed of Si and C with some Cu. This seems to be a mixture of Cu-rich phase and SiC. The presence of SiC is expected based on a combination of kinetic and thermodynamic considerations (see the discussion below). The region marked as ② in Fig. 11 is shown in more detail in Fig. 13. As shown in the micrograph, the "bulk" of the very large "square" is Cu_3Si. The composition of the phase was verified with EDS to be ~ 25 at-% of Si. However, the structure of the phase is somewhat peculiar. According to the CBED (convergent beam electron diffraction) pattern taken along the [0001] zone axis, the phase is hexagonal and not orthorhombic as suggested by Solberg.[26] However, as the hexagonal structure can be viewed as a sublattice of an orthorhombic unit cell, the entire structure can be viewed as a two-dimensional long-period superlattice composed of several domains.[26] The structure is probably best depicted as a 3x1 superlattice.[27] This observation of the somewhat unusual structure of the Cu_3Si helps one understand the XRD analyses, where it was difficult to find a good fit for the Cu_3Si peaks. The layered structure around the large "square" shows again the thin amorphous SiO_x layer on the surface. Some amorphous SiO_x is also present as spikes inside the large Cu_3Si "precipitate". No Ta_2O_5 is detected at this temperature and it is anticipated that it has been dissociated because of the formation of a-SiO_x and $TaSi_2$. Beneath the top layer, there is another layer composed of SiC grains and Cu-rich layer, which acts as a "cement" between the SiC grains. This is the same type of Cu-rich layer that was seen in Fig. 12 between the $TaSi_2$ grains and is again most likely Cu_3Si. Below this mixed layer, there is again a layer of SiC. The "flowery" pattern inside the large Cu_3Si "squares" (see Fig. 2) was also identified as $TaSi_2$.

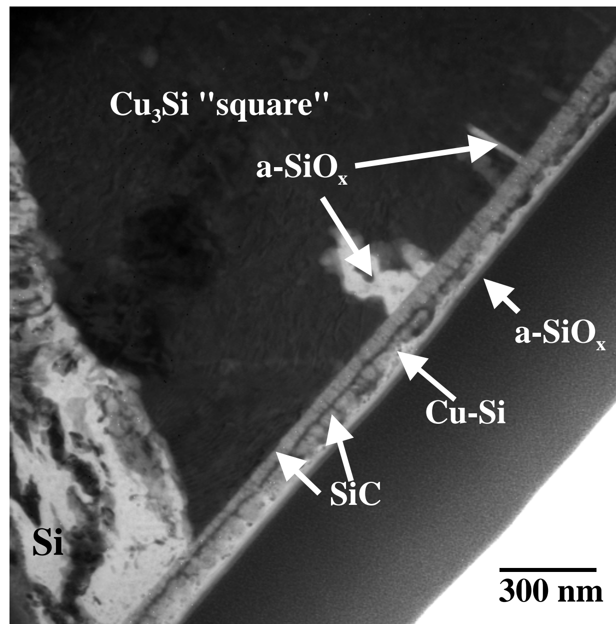

Fig.13. Bright field TEM micrograph from the Si/TaC(70nm)/Cu(400nm) sample annealed at 800 °C for 30 min corresponding to ② in Fig. 11.

IV. DISCUSSION

The "overall" stability of the TaC layers seems to be good. The Si/TaC interface in particular displays remarkable stability, since phase formation occurs only after annealing at 800 °C. However, at the TaC/Cu interface, formation of an amorphous layer takes place at a lower temperature (600 °C) than expected. The reaction is also quite abrupt, since up to 550 °C nothing else than clearly discrete layers are seen by RBS. Hence, the factors leading to the formation of the amorphous layer must be properly determined. It is argued that it is oxygen that enables the formation of the amorphous interlayer at the expense of the TaC layer at the TaC/Cu interface, which then provides an additional barrier layer against Cu diffusion. The formation of the amorphous layer is most likely caused by the presence of oxygen in the films and the diffusion of extra oxygen to the films from the annealing environment. The structure of the Cu overlayer is strongly columnar, thus providing suitable short-circuit paths for oxygen diffusion from the atmosphere during the annealings. The overall oxygen content of the as-deposited films is expected to be 1-2 at-%.[28] This is owing to the sputtering system, which is equipped with turbodrag pumps to guarantee oil

free deposition and therefore the pumping of water vapor from the chamber is not very efficient, although system has load-lock. The major part of the incorporated oxygen is most likely present at the grain boundaries of the as-deposited TaC layer, since no extensive solubility of Ta_2O_5 into TaC is expected. During the annealings oxygen dissolves into the TaC matrix from the grain boundaries.

In principle, to investigate the reactions in the present system, the thermodynamic description of the five-component Si-Ta-C-O-Cu system should be carried out. This implies the carefully assessed data on ten binary systems, ten ternary systems, and five quaternary systems. Unfortunately, there are no adequately reliable data on all the multicomponent systems required. Therefore, the reactions at the Si/TaC and TaC/Cu interfaces are examined with the help of the assessed Si-Ta-C, Ta-C-Cu and Ta-C-O ternary phase diagrams together with the calculated activity diagram for Si (Figs. 14-17), since they alone provide a considerable amount of useful information about the reactions.

The isothermal section of the metastable Ta-C-O phase diagram at 600 °C is displayed in Fig.14. The oxygen partial pressure used in the calculations was 0.2×10^{-4} Pa. Since no thermodynamic data for the metastable Ta-oxides are available, the data for stable Ta_2O_5 phase is used.[29-33] It is evident that the metastable amorphous $Ta[O,C]_x$ will eventually transform into the stable phases (i.e. Ta_2O_5 and graphite). In fact, according to the XRD-results, the formation of Ta_2O_5 took place at 725 °C (Fig. 4). When the formation of Ta_2O_5 takes place TaC and graphite must also be present, since they form a three phase field in the diagram (Fig. 14).

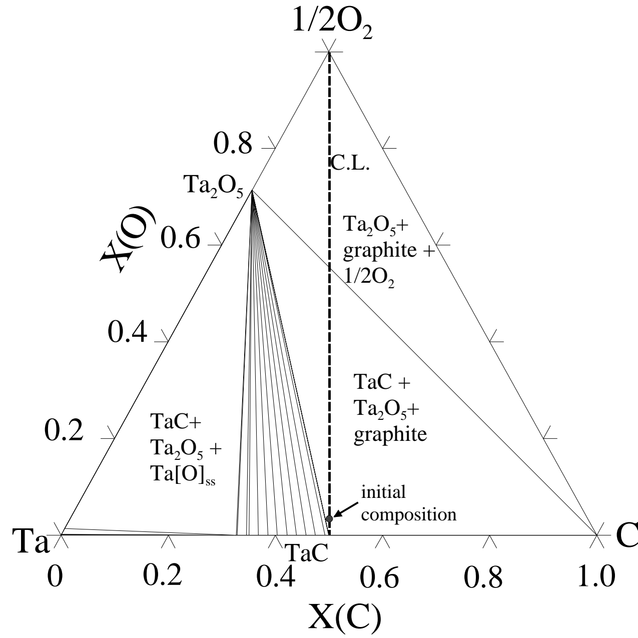

Fig. 14. Isothermal section from the evaluated metastable ternary Ta-C-O phase diagram at 600 °C under the external oxygen pressure of about 0.2×10^{-4} Pa. The tie-lines in the TaC-Ta_2O_5 two phase region are shown in the diagram. The contact-line (C.L.) between the TaC film and oxygen indicating the initial unstable equilibrium as well as the approximate composition of the $TaC[O]_{gb}$ are also shown.

TaC phase is expected to come into local equilibrium with metastable $Ta[O,C]_x$ before the formation of stable Ta_2C is possible. Therefore, the formation of Ta_2C has been suppressed in the calculations to obtain the conditions of the actual metallization structure. The initial state of the system, where the TaC is in equilibrium with the entrapped oxygen, is marked with the contact line (C.L.) in the isothermal section, showing that the situation is highly unstable. The initial composition is located on the contact line and inside the three phase field (TaC + Ta_2O_5 + graphite) in the isothermal section. Since the overall oxygen content is relatively low (~ 1-2 at-%) the composition lies close to the Ta-C binary system (the anticipated composition being depicted in Fig. 14). When the $TaC[O]_{gb}$ films are annealed at elevated temperatures, oxygen dissolves into the TaC matrix, resulting ultimately in the formation of the stable Ta_2O_5 and graphite. However, owing to the kinetic constraints, the direct formation of the stable tantalum oxide is not possible and the formation of the amorphous $Ta[O,C]_x$ layer takes place. Considering the thickness of the amorphous layer at 600 °C, it is evident that some oxygen has to be incorporated into the films also from the annealing atmosphere. Only after the temperature raises above 700 °C

the relaxation of the kinetic constraints enable the formation of the stable three phase structure (TaC + Ta_2O_5 + graphite).

The diffusion of copper can proceed only after the amorphous layer has crystallized. The crystallization of the layer occurs around 750 °C, as can be seen from Fig. 10. From the micrograph it is additionally evident that the upper part of the TaC/$Ta[O,C]_x$ bilayer is crystalline at this temperature (probably Ta_2O_5 as indicated by the XRD results in Fig. 4) and the diffusion of Cu through the barrier and the formation of Cu_3Si has taken place. Without the amorphous interlayer, the diffusion of Cu towards Si is expected to set in at much lower temperatures, since the microstructure of the TaC layer is highly columnar. Hence, the effect of oxygen is somewhat beneficial. However, the TEM micrographs displayed in Figs. 9 and 10 show clearly that approximately half of the original barrier layer is consumed by the amorphous layer before the crystallization. Hence, with thin barrier layers the amorphous layer may consume the TaC layer completely. Even though the thermal stability (i.e. the crystallization temperature) of the amorphous layer is expected to be quite high, it will change the electrical and microstructural properties of the original Si/TaC/Cu structure and can not therefore be considered beneficial. The reason for the existence of the $Ta[O,C]_x$ layer in amorphous form at relatively high temperatures, is not known. It is known, however, that metalloids, such as B, C, N, Si and P, can stabilize amorphous structure in transition metals.[34] Therefore, it is expected that carbon stabilizes the amorphous structure in this system. Carbon inhibits the crystallization of the amorphous $Ta[O,C]_x$ up to 725 °C, where the formation of Ta_2O_5 is observed (Fig. 10). No graphite could be detected at 725 °C. The reason for the absence of graphite is most probably the very difficult nucleation of the phase, as observed elsewhere.[35]

The ternary Si-Ta-C and Ta-C-Cu phase diagrams were evaluated from the assessed binary thermodynamic data[36-38], and are presented in Figs. 15 and 16. The question of carbon solubility in Ta_5Si_3, which is expected to be substantial based on the other Me_5Si_3 silicides (e.g. Ti_5Si_3 ~10 at-%)[39], must be carefully considered in the Si-Ta-C system. The question of solubility is currently a controversial topic and has not been unambiguously solved. Therefore, ternary carbon solubility into Ta_5Si_3 has not been introduced into the ternary diagram at this stage. Schuster *et al.*[40] stated that based on the investigations of

lattice parameter changes in the Ta-Si-C system, there should be no noticeable solubility of carbon into Ta_5Si_3. Instead, they propose the existence of a ternary compound $Ta_5Si_3C_{1-x}$.

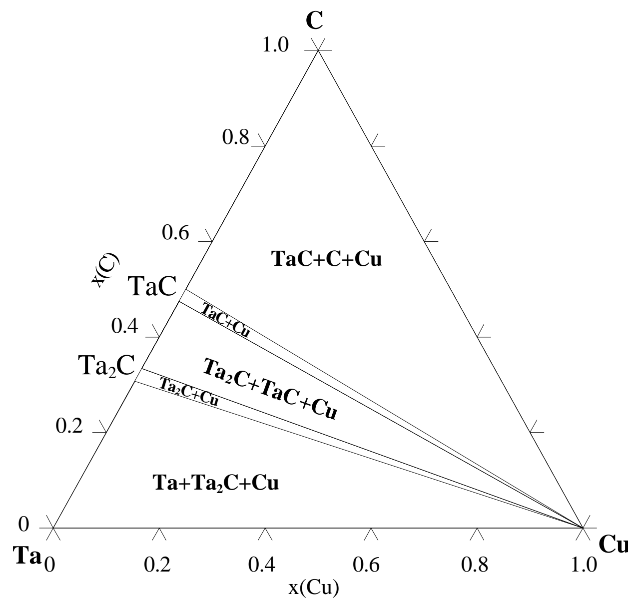

Fig.15. Isothermal section from the evaluated ternary Ta-C-Cu phase diagram at 800 °C.

The status of this compound is nevertheless still uncertain, since it is not clear if it is a real ternary compound or simply the binary Ta_5Si_3 with ternary carbon solubility. Accordingly, possible ternary compounds have similarly been excluded from the diagrams owing to the lack of reliable data. The absence of ternary phases is consistent with the general situation in the thin film systems, where ternary phases frequently have difficulties in nucleating. Nevertheless, the possible solubility of carbon into Ta_5Si_3 or the existence of ternary compounds must be experimentally verified with bulk samples, in order to establish the solubility limits and to provide a reliable basis for the understanding of these metallization systems.

It can be seen from the isothermal section of the assessed ternary Ta-C-Cu phase diagram at 800 °C (Fig. 15) that Cu is in equilibrium with both tantalum carbides TaC and Ta_2C. Thus, the TaC/Cu interface is stable, since there is no driving force for reaction between the materials. However, owing to the high affinity of Cu towards Si, it is evident that Cu will in time penetrate through the TaC layer to react with Si. Moreover, as been discussed above, oxygen incorporated into the films de-stabilizes the TaC/Cu interface and

the formation of the amorphous layer takes place. On the other hand, since the Si/TaC interface is not in equilibrium, driving force for reaction between the substrate and the TaC layer exists (Fig. 16). Assuming that the local equilibrium is achieved at the interfaces of the thin film system, it is possible to use phase diagrams coupled with certain kinetic rules to predict possible or at least to rule out impossible reaction sequences. First, the mass-balance requires that the diffusion path, which is a line in the ternary isotherm, representing the locus of the average compositions parallel to the original interface through the diffusion zone[41], crosses the straight line connecting the end members of the diffusion couple at least once. Secondly, no element can diffuse intrinsically against its own activity gradient[42] (*i.e.* from a low chemical potential area to a high chemical potential area).

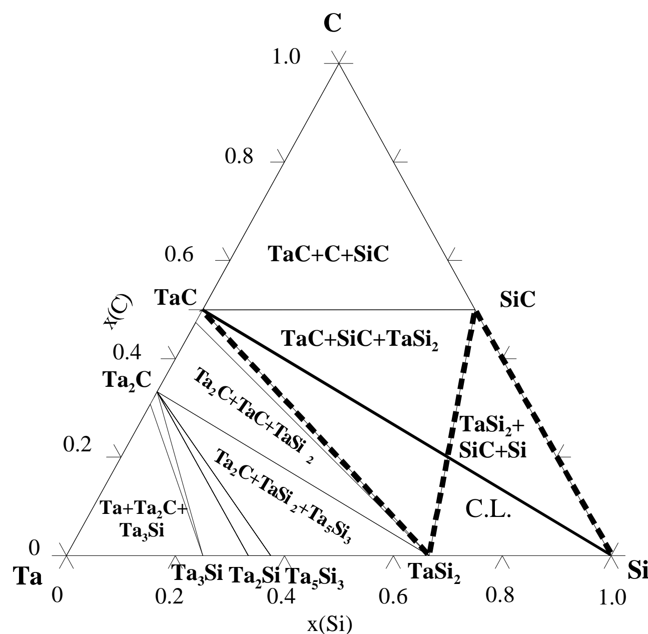

Fig.16. Isothermal section from the evaluated ternary Si-Ta-C phase diagram at 800 °C. Contact-line between Si and TaC is marked as C.L. The diffusion path is also superimposed into the isothermal section.

Although there exists a TaC + $TaSi_2$ two phase region in the phase diagram (Fig. 16), SiC must be formed to incorporate the carbon released after the formation of $TaSi_2$ in the reaction between Si and TaC, because of the mass balance requirement. The formation of SiC and $TaSi_2$ was confirmed with TEM investigations and therefore gives support to the assessed phase diagram. As shown in Fig. 12 the reacted structure consists of layers of SiC and $TaSi_2$ on top of the silicon substrate. The original TaC is used completely during the

reaction, since no traces of it can be found at 800 °C. The reaction sequence seems to be Si/SiC/$TaSi_2$/TaC, in which the TaC is used completely to yield the final structure Si/SiC/$TaSi_2$. Silicon is expected to be the first species moving at this interface because it has been found to be the mobile species during the formation of $TaSi_2$ that occurs around 650 °C in the binary Ta-Si system.[43] Further, the chemical bonding between Ta and C in the TaC compound at this essentially oxygen free interface is expected to be strong[20], and therefore Si is considered to be the only diffusing species at the Si/TaC interface around 800 °C. Whether the above presented phase formation sequence is possible, can be investigated with the help of Fig. 17. As can be seen from the calculated activity diagram, Si can move along its lowering activity gradient in the reaction sequence and the diffusion of Si is allowed on thermodynamic grounds. The reaction proceeds most likely by Si indiffusion into TaC (most probably via grain boundaries) and the following formation of $TaSi_2$, which then leads to the dissociation of TaC. The released carbon is then available for the formation of SiC in the reaction with Si. This mechanism will finally yield the experimentally observed structure Si/SiC/$TaSi_2$. Thus, carbon and tantalum would not have to move and undergo only local rearrangement. Almost identical behavior has been observed in a very similar NbC/Si diffusion couple.[44]

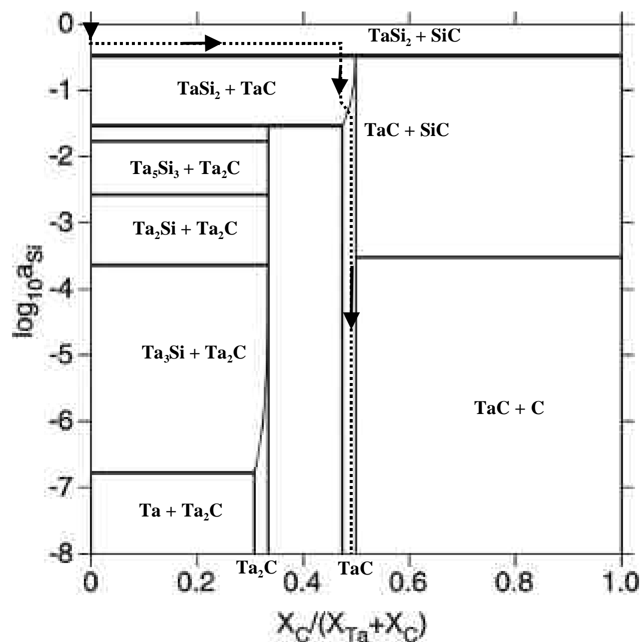

Fig.17. Potential diagram ($\log_{10}a_{Si}$ vs. $x_C/x_{Ta}+x_C$) for Si-Ta-C system at 800 °C with the superimposed diffusion path.

V. CONCLUSIONS

Interfacial reactions in the Si/TaC/Cu metallization system were investigated. The failure of the metallization structures was caused by the penetration of Cu through the TaC layer and followed by Cu_3Si formation in the case of both the thin (7-35 nm) and the thick (70 nm) TaC barrier layers. The formation of Cu_3Si was detected with XRD at 750 °C, 650 °C, and 600 °C for the 70 nm, 35 nm and 7 nm thick films, respectively. The formation of $TaSi_2$ and SiC took place at considerably higher temperatures (~ 800 °C) in the thick films giving rise to the highly complex microstructure. However, the formation of an amorphous Ta layer at the interface between TaC and Cu with noticeable amounts of carbon and oxygen was observed to take place already at 600 °C. The partial decomposition of the TaC layer due to the entrapped oxygen incorporated during the sputtering led to the formation of amorphous $Ta[O,C]_x$ layer. This emphasizes the role of oxygen in the reactions. The amorphous interlayer constitutes an additional barrier for the diffusion of Cu. The ternary Si-Ta-C, Ta-C-Cu and Ta-C-O phase diagrams were evaluated by using the assessed binary thermodynamic data. The phase relationships were found to be consistent with the experimental results. It is to be noted that in order to have more complete description of ternary systems, more experimental information on ternary solubilities is needed, particularly that of carbon in Ta_5Si_3 compound. With the help of the ternary phase diagrams and the calculated activity diagrams, the reactions taking place at the Si/barrier interface were analyzed and the sequence leading to the experimentally observed structure was explained. The Si/TaC interface was found to be stable because of the high temperatures of formation of the tantalum disilicide and silicon carbide. Based on thermodynamic considerations and experimental investigations the TaC layer seems to be a very feasible diffusion barrier, although utmost care must be excercised in processing the films.

ACKNOWLEDGEMENTS

Authors greatly acknowledge Mr. Yoshioka from JEOL and Dr. Midgley from the University of Cambridge for their contribution to the TEM analyses. The work was financially supported by the Academy of Finland.

References:

[1] P.L. Pai and C.H. Ting, IEEE Electron Device Lett., **10**, 423, (1989).

[2] M.B. Small and D.J. Pearson, IBM J. Res. Develop., **34**, 858, (1990).

[3] E. Weber, Appl. Phys. A, **30**, 1, (1983).

[4] A. Broniatowski, Phys. Rev. Lett., **62**, 3074, (1989).

[5] J. Torres, Appl. Surf. Sci., **91**, (1995).

[6] S.P. Murarka, Microelectronic Engineering, **37/38**, (1997).

[7] K. Holloway, and P. Fryer, Appl. Phys.Lett., **57,** 1736, (1990).

[8] K. Holloway, P. Fryer, C. Cabral, J. Harper, P. Bailey, and K. Kelleher, J. Appl. Phys., **71**, 5433, (1992).

[9] B-S. Kang, S-M. Lee, J. Kwak, D-S. Yoon, and H-K. Baik, J. Electrochem. Soc., **144**, 1807, (1997).

[10] D-S. Yoon, H-K. Baik, and S-M. Lee, J.Appl.Phys., **83**, 1333, (1998).

[11] L. Clevenger, N. Bojarczuk, K. Holloway, J. Harper, C. Cabral, R. Schad, F. Cardone, and L. Stolt, J. Appl. Phys., **73**, 300, (1993).

[12] T. Oku, E. Kawakami, M. Uekebo, K. Takahiro, S. Yamaguchi, and M. Murakami, Appl. Surf. Sci., **99**, 265, (1996).

[13] M.H. Tsai, S.C. Sun, C.E. Tsai, S.H. Chuang, and H.T. Chiu, J. Appl. Phys., **79**, 6932, (1996).

[14] K-H. Min, K-C. Chun, and K-B. Kim, J. Vac. Sci. Technol. , **B14**, 3263, (1996).

[15] M. Takeyama, A. Noya, T. Sase, A. Ohta, and K. Sasaki, J. Vac. Sci. Technol., **B14**, 674, (1996).

[16] J. Imahori, T. Oku, and M. Murakami, Thin Solid Films, **301**, 142, (1997).

[17] H. Tsai, S. Sun, and S. Wang, J. Electrochem. Soc.,**147**, 2766, (2000).

[18] M-A.Nicolet, Thin Solid Films, **52**, 415, (1978).

[19] T.B. Massalski, *Binary Alloy Phase Diagrams*, ASM International, (1996).

[20] H.J. Goldsmith, *Interstitial Alloys*, Butterworths, (1967).

[21] T.Laurila, K. Zeng, J.K. Kivilahti, J. Molarius and I. Suni, 2000 MRS Spring Meeting (Materials Research Society), San Francisco CA, 24-28 April, **v612**, 97, (2000).

[22] T. Laurila, K. Zeng, J. Molarius, I. Suni, and J.K. Kivilahti, J. Appl. Phys., **88**, 3377, (2000).

[23] J. Saarilahti and E. Rauhala, Nucl. Instr. and Meth. **B64**, 734, (1992).

[24] J. Saarilahti, *Ion-backscattering analysis of electronic materials*, Thesis, University of Helsinki, Acta Polytechnica Scandinavica, PH 199, Finland, (1996).

[25] J.G.M.Becht, *The Influence of Phosphorous on the Solid State Reaction Between Copper and Silicon or Germanium*, Thesis, Tech. University of Eindhoven, Netherlands, (1987).

[26] J. Solberg, Acta Cryst., **A34**, 684, (1978).

[27] P. Midgley, Private communication.

[28] T. Laurila, K. Zeng, J. Molarius, I. Suni, and J.K. Kivilahti, (submitted to Appl.Phys. Lett.)

[29] E. Gebhardt and H. D. Sehezzi, Z. Metallkd., **50**, 521, (1952).

[30] H. Jehn and E. Olzi, J. Less-Common Met., **27**, 297, (1972).

[31] S. Stecura, Metall. Trans., **5**, 1337, (1974).

[32] R. Lauf and C. Altstetter, Scr. Metall., **11,** 938, (1977).

[33] G. Boreau and P. Gerdanian, J. Phys. Chem. Solids, **42**, 749, (1981).

[34] M.A. Nicolet, in: *Diffusion in Amorphous Materials,* eds. H. Jain and D. Gupta, (TMS Warrendale, 1994), pp. 225-234.

[35] J. Burke, Acta Metall. **10**, 501 (1962).

[36] J. Lacaze and B. Sundman, Metall. Trans. A, **22**, 2211, (1991).

[37] K. Frisk and A. F. Guillermet, J. Alloys Compd., **238**, 167, (1996).

[38] L. Chandra Sekaran, SGTE databank, (1987).

[39] W. Wakelkamp, *Diffusion and Phase Relations in the Systems Ti-Si-C and Ti-Si-N*, Thesis, Tech. University of Eindhoven, Netherlands, (1991).

[40] *Phase Diagrams of Ternary Boron Nitride and Silicon Nitride Systems,* eds. P. Rogl and J.C. Schuster, ASM, (1992).

[41] J.S. Kirkaldy and L.C. Brown, Can. Met. Quat., **2**, 89, (1963).

[42] F.J.J. van Loo, Prog. Sold St. Chem., **20**, 47, (1990).

[43] A. Christou and H.M. Day, J.Electron. Mat., **5**, 1, (1976).

[44] C.R. Kao, J. Woodford and Y.A. Chang, J. Mater. Res., **11**, 850, (1996).